

# The Outer Membrane Protein OmpW Forms an Eight-stranded $\beta$ -Barrel with a Hydrophobic Channel\*

Received for publication, November 17, 2005, and in revised form, January 10, 2006. Published, JBC Papers in Press, January 12, 2006, DOI 10.1074/jbc.M512365200

Heedeok Hong<sup>‡</sup>, Dimki R. Patel<sup>§</sup>, Lukas K. Tamm<sup>‡</sup>, and Bert van den Berg<sup>§1</sup>

From the <sup>‡</sup>Department of Molecular Physiology and Biological Physics, University of Virginia, Charlottesville, Virginia 22908 and the <sup>§</sup>Program in Molecular Medicine, University of Massachusetts Medical School, Worcester, Massachusetts 01605

*Escherichia coli* OmpW belongs to a family of small outer membrane proteins that are widespread in Gram-negative bacteria. Their functions are unknown, but recent data suggest that they may be involved in the protection of bacteria against various forms of environmental stress. To gain insight into the function of these proteins we have determined the crystal structure of *E. coli* OmpW to 2.7-Å resolution. The structure shows that OmpW forms an 8-stranded  $\beta$ -barrel with a long and narrow hydrophobic channel that contains a bound *n*-dodecyl-*N,N*-dimethylamine-*N*-oxide detergent molecule. Single channel conductance experiments show that OmpW functions as an ion channel in planar lipid bilayers. The channel activity can be blocked by the addition of *n*-dodecyl-*N,N*-dimethylamine-*N*-oxide. Taken together, the data suggest that members of the OmpW family could be involved in the transport of small hydrophobic molecules across the bacterial outer membrane.

The outer membrane (OM)<sup>2</sup> of Gram-negative bacteria is a protective barrier that hinders the permeability of both hydrophilic and hydrophobic compounds, because of the presence of lipopolysaccharide (LPS) within the outer leaflet of the OM (1). To obtain nutrients and other molecules that are necessary for growth and function of the cell, Gram-negative bacteria have channels within their OM that facilitate uptake of these molecules. With respect to the transport of small, hydrophilic substances, these channels can be divided in three classes, based on their mode of transport (1): general porins, substrate-specific transporters, and active transporters. A wealth of structural and functional information is available for many of these OM channel proteins, which form monomeric or trimeric barrels that are each composed of 12–22 anti-parallel  $\beta$ -strands. In addition to OM proteins with established transport functions, the OM also contains a considerable number of smaller, monomeric  $\beta$ -barrels that are composed of 8 or 10  $\beta$ -strands. These proteins have been implicated in a wide range of functions including OM lipid metabolism, cell adhesion, and structural functions. One of these small OM proteins is OmpA from *Escherichia coli*, which belongs to a protein family with a number of established and putative functions, the most important of which is to provide structural stability to the cell via interactions of its C-terminal domain with the periplasmic pepti-

doglycan layer (1). Another member of the small OM protein family is NspA from *Neisseria meningitidis*, which belongs to the Opa family of proteins that are thought to mediate adhesion to host cells (2).

A fundamental question is whether these small barrels can function as transport channels. Arguing against this possibility are the crystal structures that have been determined for several of these proteins, and which do not show continuous channels that would be consistent with transport functions. On the other hand, it has been shown that, at least *in vitro*, OmpA forms both small and large ion channels (3) and is permeable to larger uncharged solutes (4), suggesting that the static pictures provided by the crystal structures may be misleading.

The OmpW/AlkL family (5) is a family of small OM  $\beta$ -barrel proteins for which some, albeit indirect, evidence for transport exists. The proteins belonging to this family are widespread in Gram-negative bacteria, have a length of about 200–230 amino acids, and are predicted to form 8-stranded  $\beta$ -barrels. One member of this family, OmpW from *Vibrio cholerae*, was first described more than 20 years ago and has attracted interest for vaccine development, as it is very immunogenic and seems to be present in all known *V. cholerae* strains (6–8). *E. coli* OmpW, which under normal growth conditions is expressed in only minor amounts, is a receptor for colicin S4 (9), but otherwise nothing is known about its function. Interestingly, *E. coli* OmpW shows 27% sequence identity to AlkL from *Pseudomonas oleovorans*, which is located in an operon that is dedicated to the degradation of alkanes by this organism (10). A similar degree of sequence identity is observed between *E. coli* OmpW and NahQ/DoxH, which are proteins of the naphthalene upper catabolic pathway operon that is present in several *Pseudomonas* species (11). These sequence similarities suggest an as of yet unproven role for OmpW in the transport of various hydrophobic molecules across the OM. A putative, albeit ill-defined, transport function is also suggested by the fact that growth of *Vibrio* species in the presence of high concentrations of NaCl results in a dramatic (10–20-fold) induction of OmpW, implying an involvement of this protein in osmoregulation (12, 13).

The lack of a high-resolution structure of any of the OmpW/AlkL family proteins has so far hindered attempts to assign more specific functions to members of this OM protein family. To address the question of whether OmpW homologues could form channels for the transport of small (hydrophobic) molecules, we have determined the x-ray crystal structure of OmpW from *E. coli* and performed single-channel conductance experiments of OmpW in planar lipid bilayers. The results suggest that members of the OmpW/AlkL family form channels for the transport of small (hydrophobic) compounds.

## EXPERIMENTAL PROCEDURES

**Protein Expression and Purification**—The gene for *E. coli* OmpW, including the signal sequence and with a hexa-histidine tag following the C-terminal phenylalanine residue, was amplified by PCR from genomic DNA, and cloned into the pB22 vector (14), which is under

\* This work was supported in part by National Institutes of Health Grant GM051329 (to L. K. T.). The costs of publication of this article were defrayed in part by the payment of page charges. This article must therefore be hereby marked "advertisement" in accordance with 18 U.S.C. Section 1734 solely to indicate this fact.

The atomic coordinates and structure factors (code 2F1T (trigonal) and 2F1V (orthorhombic OmpW)) have been deposited in the Protein Data Bank, Research Collaboratory for Structural Bioinformatics, Rutgers University, New Brunswick, NJ (<http://www.rcsb.org/>).

<sup>1</sup> Supported by National Institutes of Health Grant GM074824 and a PEW scholarship. To whom correspondence should be addressed: 373 Plantation St., Worcester, MA 01605. Tel.: 508-856-1201; Fax: 508-856-4289; E-mail: bert.vandenbergh@umassmed.edu.

<sup>2</sup> The abbreviations used are: OM, outer membrane; LDAO, *n*-dodecyl-*N,N*-dimethylamine-*N*-oxide; LPS, lipopolysaccharide; SIRAS, single isomorphous replacement with anomalous scattering; DPPC, dipalmitoleoyl phosphatidylcholine.

control of the arabinose promoter (15). OmpW was expressed in C43 (DE3) cells (genotype  $F^- ompT gal hsdS^B (r_B^- m_B^-) dcm lon \lambda DE3 pLys-S$  and two uncharacterized mutations described in Ref. 16) grown in 2× YT medium by induction with 0.2% arabinose for 3 h at 37 °C. After harvesting by centrifugation, the cells were resuspended in TSB buffer (20 mM Tris-HCl, 300 mM NaCl, 10% glycerol, pH 8) and ruptured by two passes at 15,000–20,000 psi in a microfluidizer (Avestin Emulsiflex C-3). Total (inner and outer) membranes were collected by centrifugation at  $131,000 \times g$  and solubilized by homogenization in 1% *n*-dodecyl-*N,N*-dimethylamine-*N*-oxide (LDAO) in TSB buffer, followed by stirring of the suspension at 4 °C for 30 min. Following centrifugation at  $131,000 \times g$ , the membrane extract derived from 12 liters of cells ( $A_{600} \sim 1.0$ ) was loaded onto a 10-ml nickel affinity column (Chelating Sepharose; Amersham Biosciences) equilibrated with 0.2% LDAO in TSB. The nickel column was washed with 20 volumes of buffer containing 5 mM imidazole and eluted with 200 mM imidazole. OmpW was further purified by gel filtration on a Superdex-200 26/60 column (Amersham Biosciences) in 10 mM sodium acetate, 50 mM NaCl, 10% glycerol, 0.05% LDAO, pH 5.5. This step was followed by cation exchange on a Resource-S column (Amersham Biosciences) equilibrated in 10 mM sodium acetate, 50 mM NaCl, 10% glycerol, 0.45% tetraethylene-mono-octylether ( $C_8E_4$ ), pH 5.5, and employing a linear NaCl gradient to 0.5 M. In addition to  $C_8E_4$ , OmpW was also purified by cation exchange in 0.05% LDAO and 1%  $\beta$ -octylglucoside. The pure protein (final yield  $\sim 5$ –10 mg per 12 liters of cells) was concentrated to 5–10 mg/ml and flash frozen in liquid nitrogen.

**Sucrose Gradient Centrifugation**—C43 (DE3) cells expressing OmpW were ruptured as described above in 20 mM Tris-HCl, 0.5 mM EDTA, pH 7.5. Cell debris was removed by centrifugation at  $10,000 \times g$  for 30 min, followed by collection of total membranes as described above. Membranes were resuspended in 4 ml of buffer and layered on a step gradient of 35–60% sucrose in buffer, with 5% increments of sucrose (10 ml each). Following centrifugation at  $131,000 \times g$  for 18 h, the two membrane fractions were drawn off, solubilized in 1% LDAO, and purified by nickel affinity chromatography as described above. OmpW was located in the heavier outer membrane fraction located at the 50–55% sucrose interface (data not shown).

**Crystallization and Data Collection**—Crystallization trials of OmpW purified in LDAO,  $\beta$ -octylglucoside, and  $C_8E_4$  were set up at 295 K by mixing 0.8  $\mu$ l of protein solution with 0.8  $\mu$ l of reservoir solutions from commercially available crystallization screens (Crystal Screen I from Hampton Research and The Classics and MbClass II screens from Nextal Biotechnologies). Whereas crystals proved difficult to obtain in  $\beta$ -octylglucoside and LDAO, OmpW purified in  $C_8E_4$  crystallized readily under various conditions. After optimization, two crystal forms were obtained that diffracted to sufficient resolution to allow collection of x-ray data. The first of these (referred to as “trigonal”) crystallized as diamonds in space group P3<sub>1</sub>21 from 28 to 32% PEG400, 0.2 M CaCl<sub>2</sub>, and 50 mM glycine, pH 9, and contained 3 molecules in the asymmetric unit ( $V_m \sim 2.8 \text{ \AA}^3/\text{Da}$ , corresponding to  $\sim 56\%$  solvent content). The diffraction from these crystals was highly anisotropic, with diffraction limits ranging from 2.4 to 3.6 Å. The second crystal form (referred to as “orthorhombic”) crystallized as bipyramids in space group P2<sub>1</sub>2<sub>1</sub>2<sub>1</sub> from 27 to 33% MPD, 0.2 M ammonium acetate, 50 mM citrate, pH 5.6, and contained 6 molecules in the asymmetric unit ( $V_m \sim 3.2 \text{ \AA}^3/\text{Da}$ , corresponding to  $\sim 62\%$  solvent content). The diffraction of these crystals was more isotropic and extended to 2.7 Å resolution. The diffraction patterns of the orthorhombic crystals could also be indexed and integrated in higher symmetry lattices (primitive cubic (P23), rhombohedral (R3), and primitive tetragonal (P4)), but subsequent scaling resulted in an

unacceptable (5–20%) number of rejections and high  $\chi^2$  values. Both crystal forms were frozen directly from the mother liquor in liquid nitrogen for data collection. Native and derivative data were collected at NSLS beamlines X25 and X6A at Brookhaven National Lab. All diffraction data were processed with HKL2000 (17).

**Heavy Atom Derivatization, Phasing, and Refinement**—Despite extensive efforts, selenomethionine-substituted protein did not yield crystals that diffracted to high resolution. Consequently, we had to solve the OmpW structure by multiple isomorphous replacement methods. Because co-crystallization approaches were not successful, a large number of heavy atom compounds were soaked into the trigonal crystals (which were obtained prior to the orthorhombic crystals). Several of the heavy atom compounds ( $K_2PtCl_4$ ,  $OsCl_3$ ) resulted in derivatives that were severely non-isomorphous with respect to the native crystals, and single anomalous dispersion and single isomorphous replacement with anomalous scattering (SIRAS) approaches did not produce useful phases. A useful derivative was eventually obtained by soaking the crystals in 2–5 mM  $YbCl_3$  for  $\sim 3$  h. A single anomalous dispersion dataset at the ytterbium peak wavelength (1.38 Å) was recorded for a derivatized crystal that diffracted to 3.2 Å resolution. Heavy atom sites (three in total; one for each molecule) were identified using SOLVE (18). Phases were obtained by SIRAS and refinement of the heavy atom sites within SHARP (19). The resulting electron density maps (after phase extension to 3.0 Å) differed greatly in quality for the three OmpW molecules within the asymmetric unit, presumably because of the anisotropy in the crystals. Initially this allowed only two of the three OmpW molecules in the asymmetric unit to be built manually, using O (20). During the course of refinement in CNS (21), the third molecule could be built as well, although its *B*-factors were much higher than those of the other two molecules. The orthorhombic crystal form was solved by molecular replacement with the program PHASER (22) implemented in ccp4 (23), using the trigonal OmpW structure as a search model. A clear solution with 6 molecules in the asymmetric unit was obtained. The model was refined in CNS as described above. During refinement of both crystal forms, it was necessary to impose tight NCS restraints on the protein to obtain acceptable  $R_{free}$  values. The data collection and refinement statistics are summarized in Table 1. Both OmpW crystal forms have good stereochemistry. Only one residue lies within the disallowed regions of the Ramachandran plot. This residue (Ser<sup>175</sup>) is present in the least well defined molecule in the asymmetric unit of trigonal OmpW (Table 1), and is located in surface loop L4 in a region with weak electron density.

**Single-channel Conductance Experiments**—Samples for single-channel recordings in planar lipid bilayers were prepared in two ways: 1) by 100-fold dilution of concentrated (8–10 mg/ml) detergent-solubilized protein in 20 mM  $C_8E_4$  buffer (OmpW: pH 5.5, 10 mM potassium acetate; OmpA: pH 9.3, 10 mM glycine; Tsx: pH 8.0, 10 mM Tris-HCl) containing 0.5 mM EDTA, and 2) by detergent removal and reconstitution into dipalmitoleoyl phosphatidylcholine (DPPC) proteoliposomes. For this, 80–100  $\mu$ g/ml of detergent-solubilized (OmpW, Tsx) or refolded (OmpA) protein prepared by method 1 was mixed with DPPC to give a final lipid concentration of 10 mM. More  $C_8E_4$  was added until the solutions became clear. The mixtures were dialyzed for 72 h (with 4 solution changes) against the corresponding detergent-free buffer. 5  $\mu$ l of protein in  $C_8E_4$  micelles or DPPC proteoliposomes were added to the *cis*- and *trans*-compartments of a bilayer setup for single-channel recordings. The two compartments, each containing 1.5 ml of 1 M KCl buffer (1 M KCl, 10 mM Tris-HCl, pH 7.3) and a chloride silver electrode, were separated by a preformed DiPhPC/decane planar bilayer in a 500- $\mu$ m hole in a Teflon partition. The *cis*-compartment was grounded while the potential was applied to the *trans*-compartment. For titration

# Structure of the Outer Membrane Protein OmpW

**TABLE 1**  
Summary of data collection and refinement statistics

	Trigonal		Orthorhombic
	YbCl <sub>3</sub>	Native	
<b>Data set and phasing statistics</b>			
Wavelength (Å)	1.38	1.10	1.10
Resolution range (outer shell) (Å)	50–3.2 (3.31–3.2)	50–3.0 (3.11–3.0)	40–2.7 (2.80–2.70)
Space group	P3 <sub>1</sub> 21	P3 <sub>1</sub> 21	P2 <sub>1</sub> 2 <sub>1</sub> 2 <sub>1</sub>
Unit cell parameters (Å, °)	82.0, 82.0, 186.3 90, 90, 120	82.2, 82.2, 186.2 90, 90, 90	118.7, 118.8, 118.5 90, 90, 120
Mosaicity (°)	0.68	0.39	0.45
R <sub>merge</sub> (%) (outer shell) <sup>a</sup>	16.3 (47.8)	7.6 (37.5)	8.7 (52.9)
Completeness (%) (outer shell)	94.5 (63.4)	98.8 (99.0)	99.5 (100.0)
I/σ (outer shell)	17.8 (2.4)	34.0 (6.1)	25.7 (4.2)
SIRAS phasing power after SHARP (iso/ano)	1.08/1.37		
SIRAS FOM after SHARP (centric/acentric)	0.32/0.41		
<b>Refinement statistics</b>			
Resolution range		8.0–3.0	8.0–2.7
Total no. atoms (non-hydrogens)		4521	8586
R <sub>work</sub> <sup>b</sup> /R <sub>free</sub> <sup>c</sup>		27.4/32.8	29.3/31.4
r.m.s. deviation <sup>d</sup> bond lengths (Å)/bond angles (°)		0.0085/1.60	0.0095/1.63
Average B-factor			
Protein (Å <sup>2</sup> )		70.1 (57.0) <sup>e</sup>	42.0
LDAO		105.6 (80.3) <sup>e</sup>	
Glycerol		61.6 (56.8) <sup>e</sup>	56.2
C <sub>8</sub> E <sub>4</sub>		88.6 (92.3) <sup>e</sup>	
% Residues in regions of Ramachandran plot			
Favored and additionally allowed/disallowed		96.0/0.2 (97.3/0.0) <sup>e</sup>	100.0/0.0

<sup>a</sup> R<sub>merge</sub> = Σ(I-1)/Σ(I).

<sup>b</sup> R<sub>work</sub> = Σ||F<sub>obs</sub> - |F<sub>calc</sub>||/Σ|F<sub>obs</sub>| for the 95% of reflection data used in refinement.

<sup>c</sup> R<sub>free</sub> = Σ||F<sub>obs</sub> - |F<sub>calc</sub>||/Σ|F<sub>obs</sub>| for the remaining 5%.

<sup>d</sup> r.m.s. deviation, root mean square deviation.

<sup>e</sup> The values between parentheses are for the best defined molecule within the asymmetric unit.

with ligands, channels were prepared by adding 5 μl of OmpW solution (200 μg/ml) reconstituted into 10 mM DPPC to both compartments. Small aliquots of 1 M arabinose or 0.25 mM LDAO stock solutions were alternately added to the *cis*- and *trans*-compartments, followed by mixing and application of +140 or -140 mV potentials. No attempts were made to reconstitute the protein unidirectionally or to determine the effect of unilateral additions of the ligands. The current fluctuation across the bilayer was filtered at 100 Hz with an 8-pole low-pass filter and recorded digitally at 1 kHz using the LABMAN program.<sup>3</sup> Single channel conductance events were analyzed interactively using IGOR software (Wave-metrics, Portland, OR) (3).

## RESULTS

**Description of the Structure**—The final trigonal OmpW model contains three protomers, three glycerols, eight C<sub>8</sub>E<sub>4</sub> molecules, and three LDAO molecules in the asymmetric unit. The entire OmpW molecule could be built, with the exception of the N-terminal histidine residue and residues Gly<sup>20</sup>–Leu<sup>28</sup> in loop L1, for which no electron density was observed. One residue of the C-terminal His<sub>6</sub> tag was visible as well. The refined orthorhombic model contains six protomers and six glycerol molecules in the asymmetric unit, and was virtually identical to trigonal OmpW (including the fact that no density was observed for residues Gly<sup>20</sup>–Leu<sup>28</sup> in loop L1). In contrast to trigonal OmpW, no unambiguous density could be observed for any detergent molecules in the orthorhombic crystals, and they were not included in the refinement. In addition, no water molecules could be assigned that resulted in lower R<sub>free</sub> values upon their inclusion during refinement, and they were not included in the final model.

The OmpW molecules are packed in both crystal forms as trimers. These are likely to be crystallographic, in view of the non-physiological orientation of the monomers relative to each other (data not shown). Supporting the monomeric arrangement in the crystals is the observa-

tion that OmpW, expressed in its native form in the *E. coli* OM, purifies as a monomer (data not shown), indicating that the protein is likely to function as a monomer.

OmpW forms an ~50-Å long 8-stranded β-barrel, with extended loops (L) on one side of the barrel and short turns (T) on the other side (Fig. 1, A and B). Because in all known OM proteins the longer loops are exposed to the extracellular surface, with the N and C terminus located in the periplasmic space, we assume that this is the case for OmpW as well. The cross-section of the barrel is ellipsoid in shape (Fig. 1C), with approximate dimensions of ~17 × 12 Å (between C<sub>α</sub> atoms) along the whole length of the barrel. The shear number (24) of the barrel is 10, making OmpW structurally similar to OmpA and NspA.

The most remarkable feature in the OmpW structure is the hydrophobic character of the interior of the barrel, as shown in Fig. 2. Of the 62 inward-pointing residues of the barrel wall, only 20 are hydrophilic (Ser, His, Asp, Glu, Asn, Gln, Arg, and Lys) and the rest are hydrophobic. The apolar character of the barrel interior extends about 30–35 Å from the extracellular exit to almost the middle of the membrane (Fig. 2), where Leu<sup>56</sup> in strand S3 and Trp<sup>155</sup> in strand S7 form a “hydrophobic gate” (Fig. 3A), closing the channel. The interior of the barrel on the periplasmic side of the gate has a more hydrophilic character, comparable with that found in most other OM proteins (Fig. 2). In this hydrophilic vestibule region, salt bridges are likely present between the residue pairs Glu<sup>54</sup>–Arg<sup>9</sup>, Arg<sup>97</sup>–Glu<sup>2</sup>, and Arg<sup>190</sup>–Glu<sup>5</sup>.

In the trigonal crystals, an elongated stretch of density is present in the center of the hydrophobic channel at the extracellular side (Fig. 3A). In the orthorhombic crystals this density, although present, is much weaker and not continuous, and for this reason we have not built anything at this site in the orthorhombic crystal form. The length of the density is consistent with an LDAO detergent molecule, which was used during the purification of the protein (see “Experimental Procedures”). The environment of the putative LDAO molecule is remarkably hydrophobic, and no polar or charged residue comes within 4 Å of the bound detergent. Instead, only the hydro-

<sup>3</sup> G. Szabo and C. Q. Ye, University of Virginia, unpublished data.

**FIGURE 1. Schematic overview of the OmpW structure.** *A* and *B*, ribbon diagrams viewed from the side, with *B*, 90° rotated relative to *A*. Extracellular loops (*L*) and periplasmic turns (*T*) are indicated. The N terminus in *B* is indicated with *N*, and the C terminus is indicated with *C*. The  $\beta$ -strands are numbered from S1 to S8. The position of the opening in the barrel wall between strands S3 and S4 is indicated with an asterisk (\*). The approximate boundary of the hydrophobic part of the OM is indicated with horizontal lines, with *out* being the extracellular environment and *in* the periplasmic space. *C*, view of OmpW from the extracellular side, showing the ellipsoidal shape of the barrel. The positions of several loops are indicated. Figs. 1, 3, and 8 were generated with PYMOL (40).

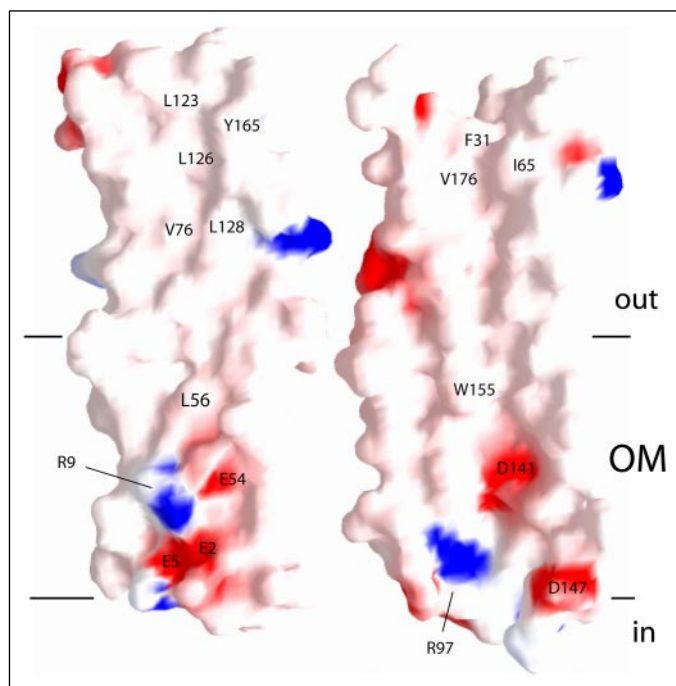
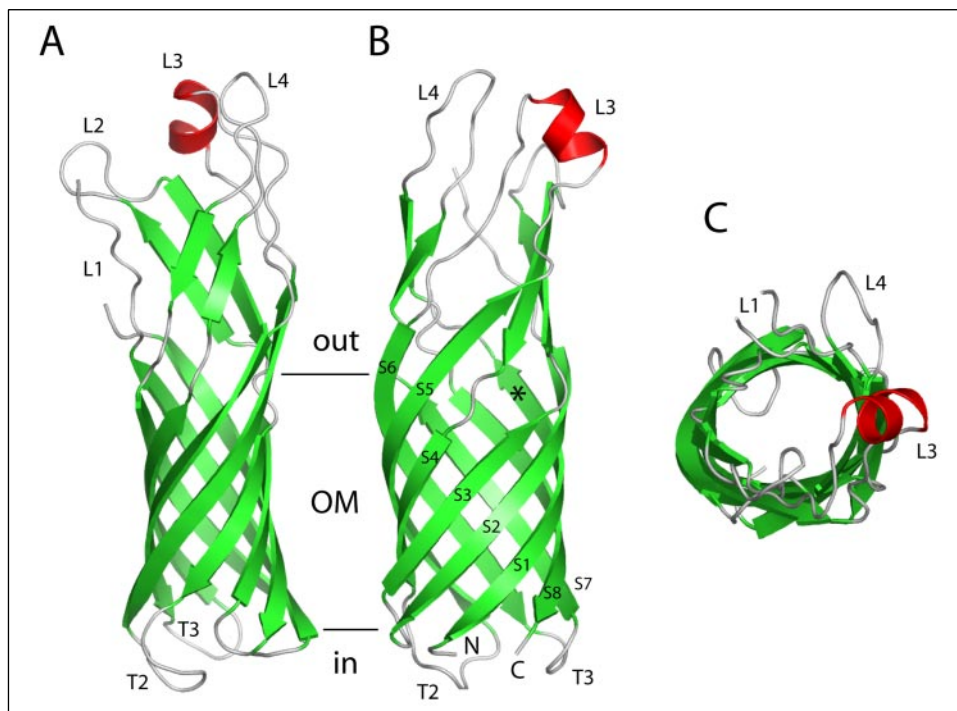


**FIGURE 2. Representations of the inside of the OmpW barrel showing the electrostatic surface potentials, with both views 180° rotated relative to each other.** The surface is colored blue for potentials  $>11$  kT/e and red for potentials  $<11$  kT/e. The side chains of selected amino acid residues are indicated with their one-letter code. The approximate positions of the hydrophobic boundaries of the OM are indicated with horizontal lines. The figure was generated with GRASP (41).

phobic residues Phe<sup>31</sup>, Ile<sup>65</sup>, Val<sup>76</sup>, Leu<sup>123</sup>, Leu<sup>126</sup>, Leu<sup>128</sup>, Tyr<sup>165</sup>, and Val<sup>176</sup> are close (within 4 Å) to the hydrophobic tail of the LDAO molecule (Fig. 3B). The polar head group of the LDAO molecule is located at the end of the barrel, and is solvent accessible (Fig. 3A). Because the LDAO molecule is still bound to OmpW after detergent exchange to C<sub>8</sub>E<sub>4</sub> (see "Experimental Procedures"), it is likely to bind in the channel with relatively high affinity.

In the periplasmic vestibule, a significant ( $\sim 5 \sigma$ ) patch of density is present at identical positions in the  $2F_o - F_c$  maps of both the trigonal and orthorhombic crystals (Fig. 3C). Both hydrophobic (Phe<sup>7</sup>, Tyr<sup>88</sup>, Leu<sup>143</sup>, and Met<sup>46</sup>) and charged residues (Glu<sup>2</sup>, Glu<sup>5</sup>, Arg<sup>9</sup>, Arg<sup>190</sup>, and Asp<sup>141</sup>) contribute to this binding pocket (Fig. 3C). Although it is not possible to identify this density unambiguously at the current resolution, we have assigned it as a molecule of glycerol for several reasons. The binding pocket is similar in character to glycerol binding sites in other proteins (for example, GlpF; Ref. 25). The hydroxyl groups of the putative glycerol molecule are close (between 2.2 and 2.8 Å) to the carboxyl groups of Glu<sup>5</sup>, Glu<sup>2</sup>, and Asp<sup>141</sup>, whereas the glycerol carbon backbone is stacked against the aromatic ring of Phe<sup>7</sup> (Fig. 3C). Supporting this assignment is the fact that inclusion of glycerol during refinement resulted in a slightly lower (0.2%)  $R_{\text{free}}$  value. This contrasts with the inclusion of a water molecule or several different cations at this site, which resulted in somewhat increased values of  $R_{\text{free}}$ . It should be noted that an arabinose molecule (and probably other pentose sugars as well) is also compatible with the density at this site, giving similar  $R_{\text{free}}$  values as for glycerol. However, because both OmpW crystal forms were purified and crystallized in the presence of 10% glycerol, the density in the binding pocket is more likely to correspond to glycerol than to arabinose.

**Single-channel Conductance Measurements**—Single-channel conductance recordings of OmpW reconstituted into planar lipid bilayers are shown in Fig. 4. Similar traces are observed when the protein is reconstituted from C<sub>8</sub>E<sub>4</sub> micelles or DPPC proteoliposomes. A statistical analysis shows that OmpW reconstituted from C<sub>8</sub>E<sub>4</sub> has a conductance of  $17 \pm 8$  pS (mean  $\pm$  S.E.) at 140 mV in 1 M KCl (determined from 279 events in two independent experiments). When reconstituted from DPPC, the conductance of OmpW is  $19 \pm 8$  pS (determined from 629 events in four experiments) (Fig. 5). Under identical conditions, OmpA has a conductance of 60–70 pS independent of the method of reconstitution (Figs. 4 and 5). These values for OmpA are similar to those reported before (3), and correspond to the formation of a small channel by the 8-stranded  $\beta$ -barrel

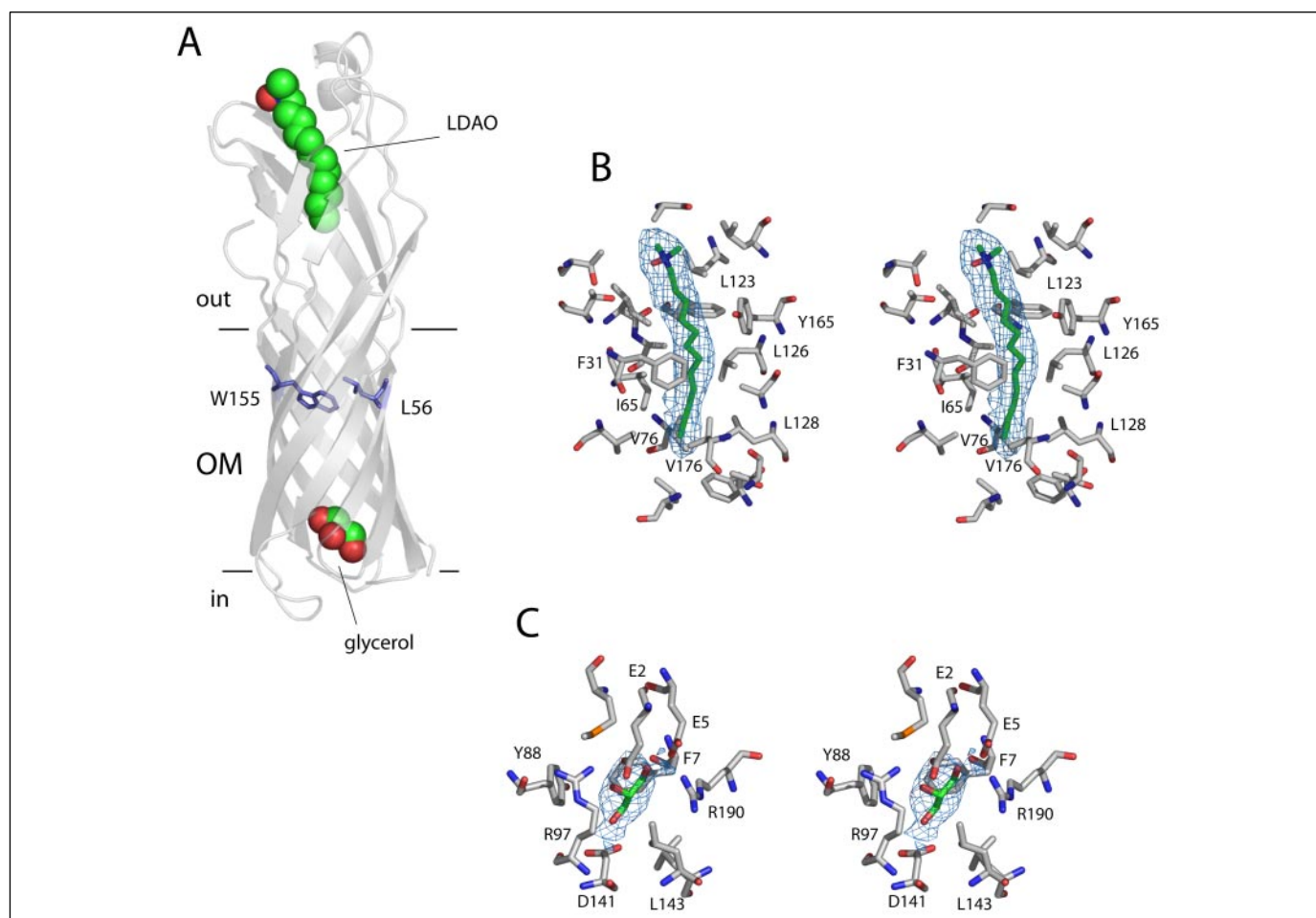


FIGURE 3. *A*, ribbon representation of OmpW viewed from the side, with the putative ligands LDAO and glycerol, as present in the trigonal crystals, indicated as CPK models. For clarity the ribbon diagram has been made transparent to show the ligands bound in the channel more clearly. The residues Leu<sup>56</sup> and Trp<sup>155</sup> that are part of the putative hydrophobic gate are shown as stick models in blue. *B*, close-up stereo diagram of the hydrophobic pocket of trigonal OmpW containing the LDAO molecule. The corresponding part of the  $2F_o - F_c$  electron density map shown is in gray, contoured at  $1.2\sigma$ . The residues that are close ( $<4\text{ \AA}$ ) to the LDAO alkyl chain are indicated with their one-letter codes. *C*, close-up stereo diagram of the putative glycerol binding site in the vestibule on the periplasmic side of the hydrophobic gate, with  $2F_o - F_c$  electron density shown as in *B*. Amino acid residues that line the binding pocket are indicated.

of the N-terminal  $\sim 176$  residues of OmpA. For comparison, we also measured the single-channel conductance of the nucleoside transporter Tsx reconstituted from  $C_8E_4$  micelles. This protein has recently been shown to form a 12-stranded  $\beta$ -barrel with a narrow central pore (26), which displays one of the smallest single-channel conductance values of any OM protein (27). The single-channel conductance of Tsx, measured under the same conditions as OmpW and OmpA is  $10 \pm 4$  pS (Figs. 4 and 5), similar to the value previously reported for this protein under the same electrolyte conditions (27).

Guided by the extra features of density present in the crystal structure, we titrated several potential ligands to DPPC-reconstituted OmpW in planar lipid bilayers to observe their effect on the conductivity of this channel. When glycerol was added up to a concentration of 135 mM ( $\sim 1.2\%$ ), no clear change in single-channel conductance behavior was observed (data not shown). The use of higher glycerol concentrations, such as those used during purification and crystallization, was not feasible because such concentrations compromised the stability of the planar lipid bilayers. By contrast, the titration of arabinose up to 20 mM resulted in an inhibition of the channel activity, as shown in Fig. 6. Analyzing several minutes worth of recording data, the open probability decreased from 33 to 9% after addition of 20 mM arabinose. It is likely that arabinose binds at the site where glycerol may be bound in the OmpW structure. At this stage, however, it is not clear if the binding of

glycerol, arabinose, or related compounds to OmpW has functional significance, because the polar vestibule residues that are likely involved in the binding of such ligands are not well conserved between OmpW homologues (Fig. 7).

When LDAO was added to OmpW, its channel activity was efficiently blocked at micromolar concentrations (Fig. 6). The open probability decreased to 0.4% after addition of  $5\ \mu\text{M}$  LDAO. This result supports our assignment of the electron density present in the extracellular part of the channel in the trigonal crystals, and reinforces our notion that LDAO binds to the channel with high affinity.

## DISCUSSION

*OmpW Contains a Deep Hydrophobic Binding Pocket*—The most interesting feature of the OmpW channel is the hydrophobic character of the major part of the barrel interior, as shown in Fig. 2. This is very unusual for OM proteins (which typically have barrel interiors that are hydrophilic and filled with water), and suggests functional significance. So far, the only known small OM proteins that have hydrophobic pockets within their barrels are the Neisserial cell adhesion protein NspA and the lipid A palmitoyltransferase PagP, the structures of which were recently solved by x-ray crystallography and NMR (2, 28–30). Both proteins have hydrophobic pockets that are occupied by a detergent molecule. The hydrophobic pocket in NspA is relatively shallow,

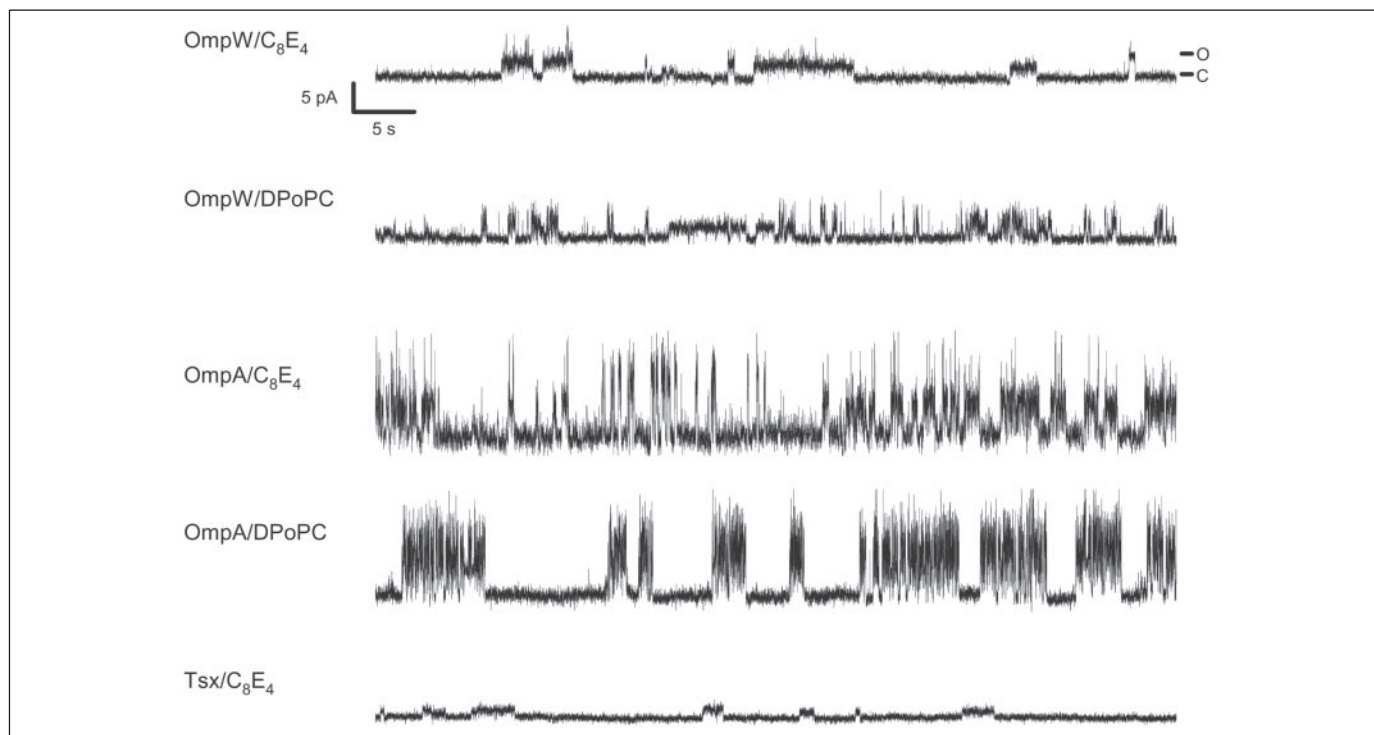


FIGURE 4. Representative single channel recordings of OmpW, OmpA, and Tsx in planar diphytanoyl-PC lipid bilayers in 1 M KCl at pH 7 and +140 mV. Proteins were reconstituted from  $C_8E_4$  detergent micelles or DPPC (DPoPC) proteoliposomes as indicated.

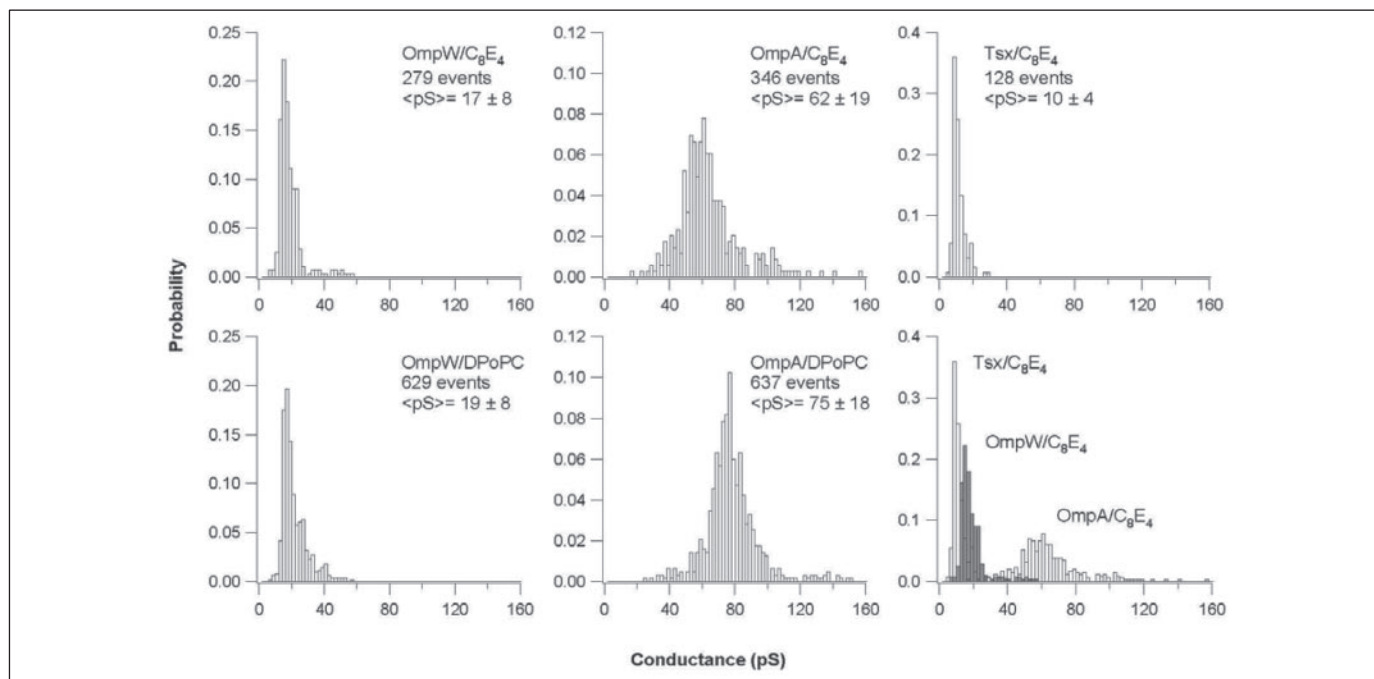


FIGURE 5. Histograms for the single-channel conductance distributions of OmpW, OmpA, and Tsx in planar lipid bilayers. The reconstitution method, total number of the identified opening events, and the mean  $\pm$  S.E. conductance values are annotated in each histogram. In the histogram at the lower right, the conductance distributions of OmpW, OmpA, and Tsx reconstituted from  $C_8E_4$  are compared directly.

located on the extracellular side at the top of the barrel, and thought to be involved in adhesion to host cell lipids. The enzyme PagP has a hydrophobic pocket inside the barrel similar to that of OmpW, although the pocket in OmpW is substantially longer. The hydrophobic pocket in PagP is thought to bind a fatty acid molecule for the subsequent transfer to lipid A during lipopolysaccharide synthesis in the OM. Consistent with this notion is the gap in the PagP barrel wall, which is thought to

provide room for the lateral entry and exit of the fatty acid in and out of the active site in exchange with the outer leaflet of the OM (28–30). By analogy with these two proteins, we consider it likely that the hydrophobic pocket of OmpW where the LDAO molecule is bound serves as a binding site for molecules that have a hydrophobic character. This notion is reinforced by the fact that the hydrophobicity of the eight residues that are located within 4 Å of the LDAO molecule is conserved

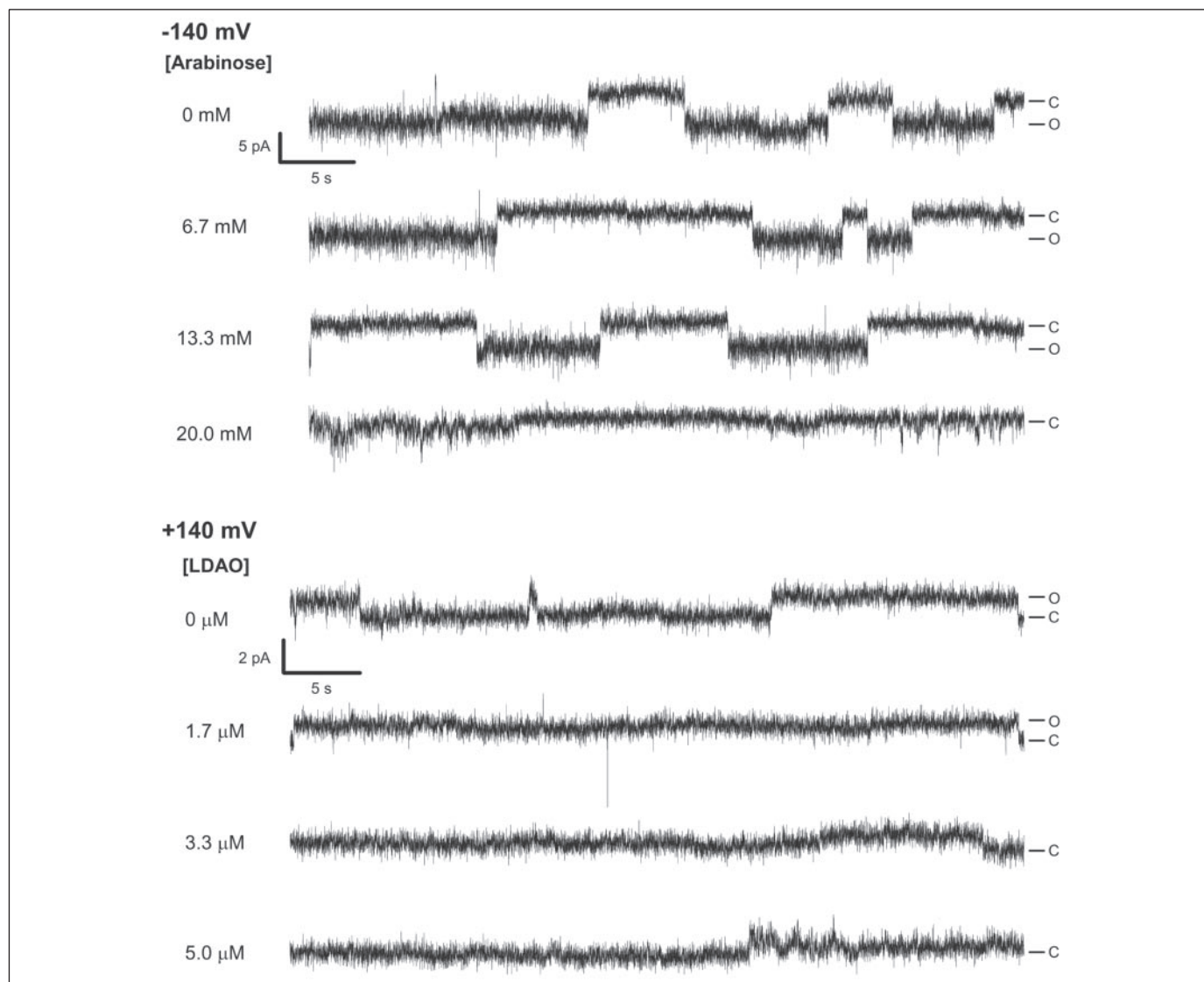


FIGURE 6. Single-channel recordings of OmpW in the presence of different concentrations of arabinose and LDAO, demonstrating the channel-blocking activity of these compounds. The OmpW channel is gradually blocked by increasing concentrations of arabinose and completely blocked by 3.3 and 5.0  $\mu\text{M}$  LDAO. A rare, very long opening event at 1.7  $\mu\text{M}$  LDAO is shown in the second trace.

between OmpW homologues, including members of the AlkL family (Fig. 7).

Whereas it seems clear that OmpW proteins can bind hydrophobic molecules that are present in the extracellular environment, it is still an open question whether OmpW, and indeed any member of the small OM protein families, could function as transporters *in vivo*. The previously determined crystal structures of the N-terminal domain of OmpA, as well as the current structures of OmpW, do not show a continuous channel spanning the entire membrane. In OmpA, this is because of the presence of a number of hydrogen bonds and salt bridges formed by polar and charged residues that line the lumen of the channel. In the case of OmpW, a continuous apolar channel that is likely to be large enough for the passage of small molecules extends all the way from the extracellular surface to the putative hydrophobic gate formed by Leu<sup>56</sup> and Trp<sup>155</sup>, located approximately halfway through the membrane (Figs. 3 and 8). On the periplasmic side of the gate, interactions between polar and charged residues are responsible for the closed state of the OmpW channel observed in the crystal structures. However, previous results (3) and the present single channel data for OmpW and

OmpA strongly suggest that these proteins form ion channels *in vitro*. As argued before (3), this indicates that the interiors of these proteins are much more dynamic than is evident from the static x-ray crystallographic structures, which do not show continuous channels. In accord with this notion, conformational exchange on the  $\mu\text{s}$  to ms time scale of several barrel residues of OmpA has been observed by NMR (31). Molecular dynamics simulations also suggest that the side chains of residues in the putative channel of OmpA are mobile enough to, at least transiently, allow the formation of a transport pore (32). Thus, whereas OmpA has several functions that are not transport-related, accumulating data suggest that it may be involved in transport as well.

*OmpW Forms a Hydrophobic Channel*—The single channel conductance of OmpW in 1 M KCl and at  $\pm 140$  mV is about 18 pS. This is a three to four times smaller value than that of OmpA under the same conditions (Fig. 5). The smallest OM protein that is known to form a *bona fide* transport channel is the nucleoside transporter Tsx, which has a 12-stranded  $\beta$ -barrel with a small central pore that crosses the entire width of the membrane (26). Interestingly, under conditions identical to those employed for OmpW and OmpA, we measured a single channel

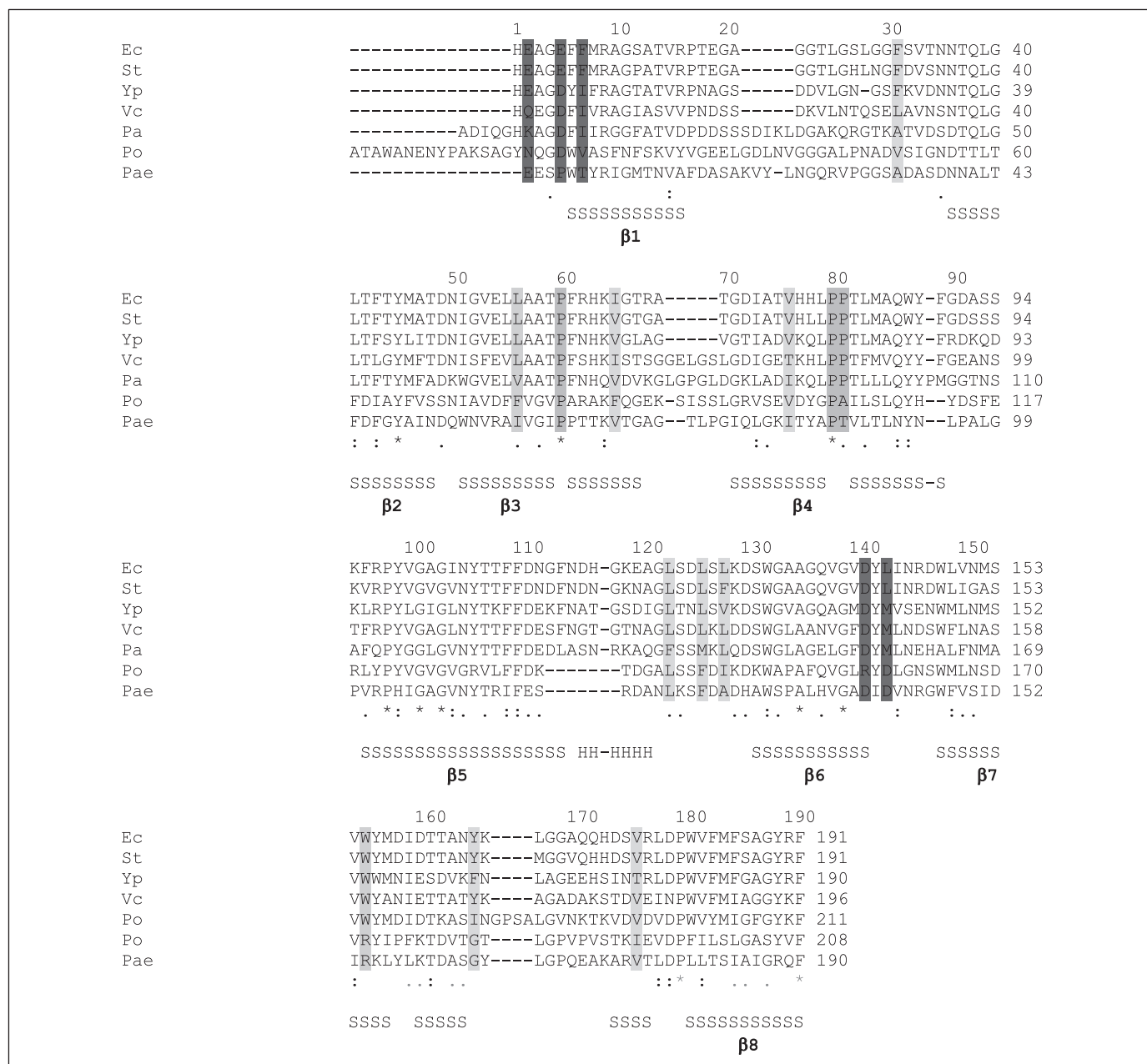


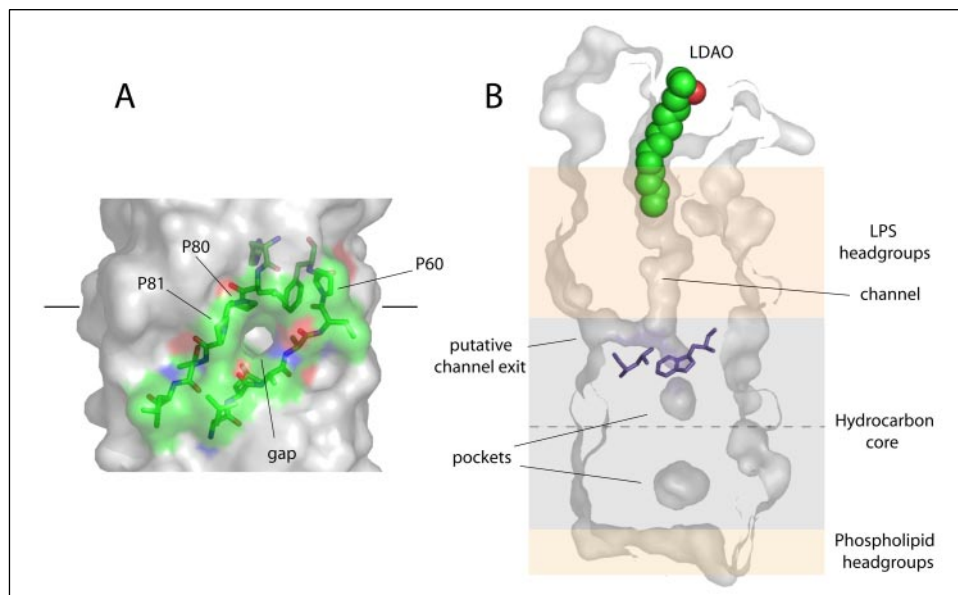
FIGURE 7. Clustal alignment of OmpW/AikL homologs. Residues that are close ( $<4 \text{ \AA}$ ) to the glycerol molecule are shown in dark gray, those that are close to the LDAO molecule in light gray. The proline residues that are part of the gap in the barrel wall between strands S3 and S4 are shown in gray. The two residues (Leu<sup>56</sup> and Trp<sup>155</sup>) of the hydrophobic gate are shown in gray. The observed secondary structure of *E. coli* OmpW as determined with the program DSSP (42) is shown at the bottom, with  $\beta$ -strands represented with S and the  $\alpha$ -helix in loop L3 with H. The transmembrane strands are indicated and numbered with  $\beta$  in bold. The following proteins were aligned: *Ec*, *E. coli* OmpW; *St*, *S. typhimurium* OmpW; *Yp*, *Yersinia pestis* OmpW; *Vc*, *V. cholerae* OmpW; *Pa*, *Pseudomonas aeruginosa* OprG; *Po*, *P. oleovorans* AikL; *Pae*, *Pseudomonas aeruginosa* NahQ.

conductance value of only 10 pS for Tsx (Fig. 5), confirming results from a previous study (33) and demonstrating that the permanently open pore of Tsx gives rise to smaller conductance values than the transient pores of OmpA and OmpW. The very small conductance values measured for the nucleoside transporter provide, in our opinion, a strong argument that the larger conductance measured for OmpW and OmpA are the result of the formation of *bona fide* channels by these proteins. The much lower ion permeability of the OmpW relative to the OmpA channel is likely because of the lining of the interior of the OmpW channel with hydrophobic residues as opposed to hydrophilic residues, which would make the passage of ions energetically more favorable in the case of OmpA. In addition, there may also be differences in pore diameter or side chain dynamics between the two channels.

Recent data for OmpW homologs suggest that members of this protein family may be involved in bacterial adaptation in response to various stress conditions. Proteomic analysis of *Stenotrophomonas* sp. OK-5 revealed that OmpW is, together with stress-shock proteins such as DnaK and OsmC, one of the few proteins that become significantly induced by the presence of trinitrotoluene in the growth media (34). In another report, the expression of OmpW from *V. cholerae* was found to be dependent on *in vitro* culture conditions such as temperature, salinity, and availability of nutrients or oxygen (35). The expression of the OmpW homolog from *Vibrio alginolyticus*, a marine pathogen, was induced dramatically (at least 10-fold) under conditions of high salinity (4% NaCl), implying a role of OmpW in osmoregulation (12, 13). Although these data imply a transport function for OmpW family

## Structure of the Outer Membrane Protein OmpW

FIGURE 8. *A*, transparent surface view of OmpW, showing the gap in the barrel wall between strands S3 and S4. Residues 55–61 of strand S3 and residues 78–83 of strand S4 are shown as stick models, with carbon atoms colored green, oxygen red, and nitrogen blue. The proline residues Pro<sup>60</sup> (P60), Pro<sup>80</sup> (P80), and Pro<sup>81</sup> (P81) are indicated. The approximate boundary of the hydrophobic part of the OM on the extracellular side is shown as horizontal lines. *B*, cross-section of OmpW viewed from the side, 90° rotated relative to *A*, showing the internal surface of the hydrophobic channel with the bound LDAO molecule (shown as a CPK model) and several pockets on the periplasmic side of the hydrophobic gate, which are presumably filled with water. The putative channel exit site that is present at the apolar hydrocarbon-polar head group interface of the LPS monolayer in the OM is indicated. The residues Leu<sup>56</sup> and Trp<sup>155</sup> forming the hydrophobic gate are shown in blue as stick models.



members, it is clear that such a broad regulation of protein expression by a number of external stress factors hampers efforts to assign more specific functions to these proteins. As an example, based on the observation that OmpW expression was dramatically decreased in a ceftriaxone-resistant strain of *Salmonella typhimurium*, it was recently proposed that OmpW might be involved in the uptake of this antibiotic (36). Based on our structure, however, it is unlikely that this relatively large (660 Da) and polar molecule would be able to traverse the OM through the OmpW channel.

Although the currently available data suggest that members of the OmpW family function as transporters under various stress conditions, the identities of the putative substrates that are transported by OmpW proteins are not yet clear. The hydrophobic character of the interior of the OmpW channel, the presence of LDAO in the crystal structure, and the blockage of the channel activity observed with LDAO, make small hydrophobic molecules the most likely transport substrates of OmpW channels. Moreover, although we cannot exclude a role for OmpW in the export of (toxic) molecules from the cell, the presence of a well defined hydrophobic binding pocket on the extracellular side of the membrane makes an import function much more likely. The sequence similarity of OmpW and AlkL/NahQ further supports the role of OmpW proteins as transporters of hydrophobic molecules. However, it is clear that, even though AlkL may be involved in alkane transport in *Pseudomonas* species, alkanes are only metabolized by certain species of Gram-negative bacteria. For this reason, OmpW channels are unlikely to function as general facilitators of alkane transport. So far, experiments designed to demonstrate the involvement of the putative alkane transporter AlkL from *P. oleovorans* in alkane uptake are inconclusive because *alkl* knock-out strains were able to grow on octane as the sole carbon source.<sup>4</sup> However, this negative result can be explained by a redundancy in OM transport systems for these compounds. For example, members of the FadL family of long-chain fatty acid/xenobiotics transporters (37, 38) are present in all *Pseudomonas* species sequenced to date, and it is likely, although not yet proven, that these proteins can also transport hydrophobic molecules other than long-chain fatty acids, such as alkanes. In addition, *alkl*, like the other *alk* genes, is plasmid encoded, and a chromosomally encoded OmpW homologue is likely to

exist in *P. oleovorans*. Therefore, future experiments designed to demonstrate involvement of OmpW/AlkL family proteins in the uptake of alkanes or other hydrophobic molecules should be carried out in a *fadL/ompw* knock-out strain.

*A Possible Mechanism for Transport of Hydrophobic Compounds by OmpW*—As has been shown for long-chain fatty acids (39), amphiphilic and hydrophobic molecules readily pass through regular phospholipid bilayers, making dedicated transport systems in principle not necessary for such membranes. However, the bacterial OM is an unusual biological membrane in the sense that it contains LPS as the principal component in the outer leaflet (1, 37). The sugar moieties of the LPS form a polar layer on the outside of the cell, which is the reason why amphiphilic and hydrophobic compounds do not easily pass through that layer. By contrast, the hydrocarbon region of the OM is unlikely to present a major permeability barrier for these compounds. Taking this into consideration, the current crystal structure suggests an intriguing transport model. OmpW possesses a continuous passageway that leads from the extracellular surface where the LDAO molecule is bound, to a gap that is present in the barrel wall between residues Leu<sup>56</sup>–Phe<sup>61</sup> of strand S3 and residues His<sup>77</sup>–Pro<sup>81</sup> of strand S4 (Figs. 1B and 8). Importantly, the gap is located close to the extracellular belt of aromatic residues (not shown), likely placing it at the hydrophilic/hydrophobic interface of the outer leaflet of the OM. The gap as present in the structure seems wide enough to allow for a lateral passage of small hydrophobic molecules into the lipid bilayer. It is notable that three proline residues, Pro<sup>60</sup>, Pro<sup>80</sup>, and Pro<sup>81</sup>, are located in the immediate vicinity of the barrel gap. Although only Pro<sup>80</sup> is absolutely conserved between OmpW homologues, the other two prolines are also fairly well conserved and are present in the majority of OmpW sequences (Fig. 7). These prolines may help to stabilize the unusual conformation of strands S3 and S4 in this region, preventing the formation of interstrand hydrogen bonds and enabling the formation of a gap in the barrel wall. Thus, hydrophobic molecules could bypass the polar part of the LPS layer by diffusing down the hydrophobic channel and moving laterally through the gap in the barrel wall into the OM. Substrate molecules could then diffuse or flip to the inner layer of the OM, followed by diffusion into and across the periplasm, possibly assisted by periplasmic binding proteins. The alternative to this lateral exit model would be a more classical mechanism, in which the substrate could diffuse down the entire length of the barrel to

<sup>4</sup> J. van Beilen, unpublished results.

reach the periplasm. In this transport mechanism, the substrate would need to pass through the vestibule on the periplasmic end of the OmpW channel (Fig. 2), which is filled with polar side chains, some of which form salt bridges in our structure. However, the observed single channel activities of OmpW, together with the fact that the channel activity is blocked by a substrate that likely binds in the vestibule, shows that polar molecules such as ions traverse the OmpW barrel in the classical way. Site-directed mutagenesis experiments, for example, targeting the proline residues in the vicinity of the barrel gap or eliminating the salt bridges in the polar vestibule, could provide a means to distinguish between the lateral exit model and the classical transport model. To do this, however, transport substrates for the OmpW channels will have to be identified first, and this will be the focus of future experiments.

*Acknowledgments*—We are grateful for the generosity and support of Tom Rapoport (Harvard Medical School) at whose laboratory this project was initiated, also to Vivian Stojanoff, Marc Allaire, and Jean Jakoncic from beamline X6A of the National Synchrotron Light Source (NSLS) for beamtime and beamline support, and Gabor Szabo (University of Virginia) for use of the planar lipid bilayer equipment.

## REFERENCES

- Nikaido, H. (2003) *Microbiol. Mol. Biol. Rev.* **67**, 593–656
- Vandeputte-Rutten, L., Bos, M. P., Tommassen, J., and Gros, P. (2003) *J. Biol. Chem.* **278**, 24825–24830
- Arora, A., Rinehart, D., Szabo, G., and Tamm, L. K. (2000) *J. Biol. Chem.* **275**, 1594–1600
- Sugawara, E., and Nikaido, H. (1992) *J. Biol. Chem.* **267**, 2507–2511
- Busch, W., and Saier, M. H., Jr. (2003) *Methods Mol. Biol.* **227**, 21–36
- Jalajakumari, M. B., and Manning, P. A. (1990) *Nucleic Acids Res.* **18**, 2180
- Das, M., Chopra, A. K., Cantu, J. M., and Peterson, J. W. (1998) *FEMS Immunol. Med. Microbiol.* **22**, 303–308
- Soderblom, T., Oxhamre, C., Wai, S. N., Uhlen, P., Aperia, A., Uhlin, B. E., and Richter-Dahlfors, A. (2005) *Cell. Microbiol.* **7**, 779–788
- Pilsel, H., Smajs, D., and Braun, V. (1999) *J. Bacteriol.* **181**, 3578–3581
- Van Beilen, J. B., Eggink, G., Enequist, H., Bos, R., and Witholt, B. (1992) *Mol. Microbiol.* **6**, 3121–3136
- Eaton, R. W. (1994) *J. Bacteriol.* **176**, 7757–7762
- Xu, C., Ren, H., Wang, S., and Peng, X. (2004) *Res. Microbiol.* **155**, 835–842
- Xu, C., Wang, S., Ren, H., Lin, X., Wu, L., and Peng, X. (2005) *Proteomics* **5**, 3142–3152
- Van den Berg, B., Clemons, W. M., Jr., Collinson, I., Modis, Y., Hartmann, E., Harrison, S. C., and Rapoport, T. A. (2004) *Nature* **427**, 36–44
- Guzman, L. M., Belin, D., Carson, M. J., and Beckwith, J. (1995) *J. Bacteriol.* **177**, 4121–4130
- Miroux, B., and Walker, J. E. (1996) *J. Mol. Biol.* **260**, 289–298
- Otwinowski, Z., and Minor, W. (1997) *Methods Enzymol.* **307**–326
- Terwilliger, T. C., and Berendzen, J. (1997) *Acta Crystallogr. Sect. D* **55**, 849–861
- de La Fortelle, E., and Bricogne, G. (1997) *Methods Enzymol.* **276**, 472–494
- Jones, T. A., and Kjeldgaard, M. (1997) *Methods Enzymol.* **277**, 173–207
- Brunger, A. T., Adams, P. D., Clore, G. M., DeLano, W. L., Gros, P., Grosse-Kunstleve, R. W., Jiang, J. S., Kuszewski, J., Nilges, M., Pannu, N. S., Read, R. J., Rice, L. M., Simonson, T., and Warren, G. L. (1998) *Acta Crystallogr. Sect. D* **54**, 905–921
- Read, R. J. (2001) *Acta Crystallogr. Sect. D* **57**, 1373–1382
- The CCP4 Suite: Programs for Protein Crystallography (1994) *Acta Crystallogr. Sect. D* **50**, 760–763
- Schultz, G. E. (2002) *Biochim. Biophys. Acta* **1565**, 308–317
- Fu, D., Libson, A., Miercke, L. J., Weitzman, C., Nollert, P., Krucinski, J., and Stroud, R. M. (2000) *Science* **290**, 481–486
- Ye, J., and van den Berg, B. (2004) *EMBO J.* **23**, 3187–3195
- Benz, R., Schmid, A., Maier, C., and Bremer, E. (1988) *Eur. J. Biochem.* **176**, 699–705
- Ahn, V. E., Lo, E. I., Engel, C. K., Chen, L., Hwang, P. M., Kay, L. E., Bishop, R. E., and Prive, G. G. (2004) *EMBO J.* **23**, 2931–2941
- Hwang, P. M., Choy, W. Y., Lo, E. I., Chen, L., Forman-Kay, J. D., Raetz, C. R., Prive, G. G., Bishop, R. E., and Kay, L. E. (2002) *Proc. Natl. Acad. Sci. U. S. A.* **99**, 13560–13565
- Hwang, P. M., Bishop, R. E., and Kay, L. E. (2004) *Proc. Natl. Acad. Sci. U. S. A.* **101**, 9618–9623
- Tamm, L. K., Abildgaard, F., Arora, A., Blad, H., and Bushweller, J. H. (2003) *FEBS Lett.* **555**, 139–143
- Bond, P. J., Faraldo-Gomez, J. D., and Sansom, M. S. (2002) *Biophys. J.* **83**, 763–775
- Maier, C., Bremer, E., Schmid, A., and Benz, R. (1988) *J. Biol. Chem.* **263**, 2493–2499
- Ho, E. M., Chang, H. W., Kim, S. I., Kahng, H. Y., and Oh, K. H. (2004) *Curr. Microbiol.* **49**, 346–352
- Nandi, B., Nandy, R. K., Sarkar, A., and Ghose, A. C. (2005) *Microbiology* **151**, 2975–2986
- Hu, W. S., Li, P. C., and Cheng, C. Y. (2005) *Antimicrob. Agents. Chemother.* **49**, 3955–3958
- Van den Berg, B. (2005) *Curr. Opin. Struct. Biol.* **15**, 401–407
- Van den Berg, B., Black, P. N., Clemons, W. M., Jr., and Rapoport, T. A. (2004) *Science* **304**, 1506–1509
- Hamilton, J. A. (2003) *Curr. Opin. Lipidol.* **14**, 263–271
- DeLano, W. L. (2002) *The PyMOL User's Manual*, DeLano Scientific, San Carlos, CA
- Nicholls, A., Sharp, K., and Honig, B. (1991) *Proteins Struct. Funct. Genet.* **11**, 281–296
- Kabsch, W., and Sander, C. (1983) *Biopolymers* **22**, 2577–2637